Numerical simulation of upward flame spread over vertical combustible surface

E. S. Kokovina[1], E. A. Kuznetsov, A. Yu. Snegirev

Saint Petersburg Peter the Great Polytechnic University, St. Petersburg, Russia

Abstract

This paper explores capability of FDS 6.4 to accurately predict upward flame spread over vertical surfaces of a non-charring polymer (PMMA) material and examines the regimes of flame propagation depending on the ignitor properties and availability of side walls. The necessary grid requirement is elaborated by replicating heat flux measurements for flames attached to a vertical wall. It is demonstrated that the flame propagation regime is very sensitive to how the material is ignited. Three qualitatively different flame spread regimes with necking, parabolic and V-shaped pyrolysis zones have been observed, depending on the ignitor power and size and the pathway of side air entrainment.

1. Introduction

Dynamics of flame propagation over combustible surfaces is known to be affected by: (1) orientation of the burning surface, (2) propagation direction relative to airflow, (3) spatial scale and flow regime, (4) sample thickness, (5) material type. This work focuses on large-scale turbulent flames adjacent to and propagating upwards along the vertical plane surfaces of a non-charring material.

Current practice of flame spread modelling can be classified depending on the flame and solid phase sub-models used. In flame modeling, heat flux incident at the burning surface can be either prescribed based on the empirical data [1–3, 7] or evaluated by

[1] Corresponding author: kokovinae@gmail.com
Department of Fluid Dynamics, Combustion and Heat Transfer
Institute of Applied Mathematics and Mechanics
Polytechnicheskaya 29, St.-Petersburg, 195251, Russia

means of a CFD model [4–6, 8, 9]. It is worthy of note that relative distribution of the total surface heat flux between radiative and convective components depends on spatial scale. In solid phase modeling, ignition temperature and burning rate are either prescribed [1–5] or evaluated by a pyrolysis model [6–10].

Simple analytical models are designed to predict propagation of the pyrolysis zone based on the empirical relations for the flame length [1–3]. These models, however, do not allow for the curvature of the pyrolysis front.

In CFD modeling, thermal feedback between solid phase pyrolysis and gaseous flame is considered. In earlier works (for example see [4, 5]), a simplified consideration of pyrolysis was employed. Within this approach, combustible material is assumed inert while warming up to a prescribed value of the surface temperature (ignition temperature). As the ignition temperature is reached, the surface temperature remains unchanged, and pyrolysis proceeds at a constant prescribed rate. A more comprehensive approach used in [6, 8, 9] utilizes a pyrolysis model with the pyrolysis rate depending on material temperature and conversion.

Despite recent advances, coupled simulations of flame spread over the surface of a combustible material remain extremely challenging, particularly when performed in realistic fire scenarios. Indeed, while certain successful attempts to predict flame spread with the in-house software can be found in literature [8, 9], convincing examples of using Fire Dynamics Simulator (FDS) to predict flame spread are limited. In particular, Ref. [6] attempts to replicate experimental data and shows considerable discrepancies between the measurements and predictions. This is mainly due to inaccuracy of predicting both surface heat flux and pyrolysis rate. As such, validation of the model and code is required in both uncoupled (prescribed fuel supply rate) and coupled (sample burning rate is determined by the surface heat balance) modes.

The main objective of this work is to develop FDS-based methodology for prediction of upward flame spread. To meet this objective, two distinct tasks are addressed. Firstly, FDS is validated in the uncoupled mode against the vertical wall fire case [11] in order to evaluate the effect of grid resolution on predicted flame heat flux to the solid surface. Secondly, the experimental scenario [12] of vertical upward flame spread is considered, and the flame propagation dynamics is predicted. The specific objectives of this study is identification of the flame propagation regimes with distinct patterns of pyrolysis front due to the effect of igniter shape/size/temperature as well as the effect of side air entrainment.

2. Model description

FDS [13] is an open-source CFD tool developed to predict fire dynamics, in which the Navier-Stokes equation system is solved in the low-Mach number limit. The large eddy simulation approach (LES) is used to simulate turbulent flow. To model subgrid turbulence, the Deardorff's model is applied. Large-eddy simulations of boundary layer flows performed by FDS fall in the category of LES with near-wall modeling; the standard log-law wall functions with the Van Driest damping are employed. Convective heat flux at the solid surface is calculated as $q_w'' = h(T - T_w)$, where T_w is the wall surface temperature, T is the resolved temperature in the near-wall cell, and the heat transfer coefficient, h, is estimated using the empirical correlation for buoyant flows.

For turbulent combustion modeling, the eddy dissipation concept is utilized at the subgrid level, and the single-step fast irreversible reaction is considered. A constant soot yield per unit mass of burnt fuel is assumed. The rate of fuel consumption is set proportional to both the local limiting reactant concentration and the local rate of mixing. The reaction time scale is set minimum of diffusion, subgrid turbulent mixing, and buoyancy time scales.

Radiative transfer is simulated by solving the radiative transfer equation using the finite volume method with 104 discrete solid angles. Spectral properties of the gas-soot media are accounted for by the mean (gray) absorption coefficients, which are simulated by the RadCal procedure as a function of composition and temperature. The ratio of the radiation emission to the chemical heat release in a grid cell is set equal to the pre-assumed value called radiative fraction (this quantity is material dependent).

1D heat transfer equation is solved in the material layer in the direction normal to the exposed fuel surface. Boundary condition at the fuel surface takes into account conductive heat transfer to the material, absorbed radiation, reradiation, and the convective heat flux from the gas phase. Transparency of the material for the radiative flux is accounted for. The pyrolysis model assumes single-step first-order reaction of Arrhenius type.

3. Simulation results

3.1. Vertical wall fire

In this section, the effect of grid resolution on the surface heat flux from flame adjacent to the vertical wall is addressed in uncoupled mode. The experimental data by FM Global [14] are used to validate the model. Recently published paper [11] provides FireFOAM simulation results for the same scenario; these results are also used for comparison.

Gaseous fuel (propylene) is uniformly supplied through the vertical burner surface (0.792 m height, 0.38 m width) at a rate of 17.1 $g/(m^2 \cdot s)$. Thermal properties of propylene are taken as the default values implemented in FDS (in particular, heat of combustion equals to 49 MJ/kg), except for radiative fraction, which is set to 0.25 for consistency with Ref. [11].

The computational domain (1.512 m high, 0.8 m deep and 0.38 m wide) is shown in Fig. 1. Two 12 cm wide adiabatic side walls are attached to the surface at which gaseous fuel is supplied. Boundaries beyond the side walls, as well as bottom, front and top boundaries are open. The computational domain is extended by 6 cm below the bottom of the burner surface. The burner surface and the solid inert wall below and above the burner are kept at 75 °C.
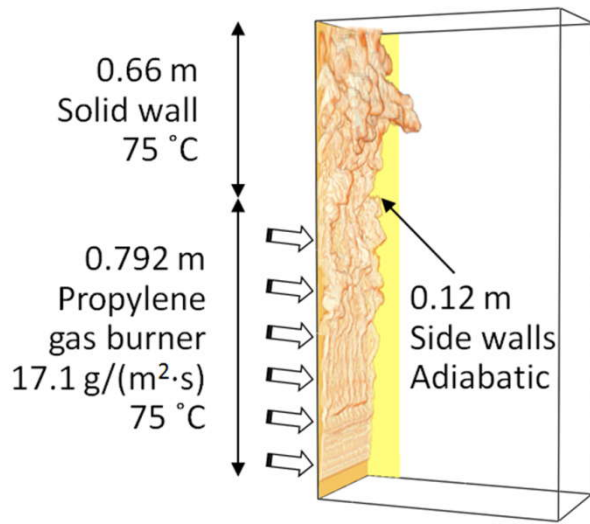
Fig. 1. Computational domain and boundary conditions. Only one of two side walls is shown. Transparent surfaces of the domain are the open boundaries. Also shown is the instantaneous iso-surface of heat release rate (200 kW/m^3) visualizing the flame shape

Multi-block Cartesian grids were used in the simulations. Measurements [14] and estimates made in [11] show that the viscous sub-layer thickness in the buoyant near-wall flow is of order of 1 mm. Keeping it in mind, several grid resolutions are considered with the sizes of the near-wall grid cells normally to the wall surface equal to 15, 10, 5, 3 and 2 mm. The grid is uniform up to 0.12 m away from the wall surface and is stretched in the wall-normal direction afterwards. The total number of grid cells varies from 13 650 to 3 578 232 for the above values of grid cell sizes.

The grids are similar to those used in Ref. [11], where simulations were performed by FireFOAM software in which WALE (Wall-Adapting Local Eddy-viscosity) near-wall model was applied and compared to the one-equation model. Dissimilar to that, the log-law wall functions with the Van Driest damping were used in this work. As shown in Fig. 2, a, it results in the subgrid kinetic energy vanishing at the wall (as well as the eddy viscosity), which is qualitatively similar to the FireFOAM

predictions by the WALE model (note, that FireFOAM prediction by the one-equation model shown by the dashed line is qualitatively incorrect in the near-wall region). However, the magnitude of the subgrid kinetic energy obtained in this work differs greatly from FireFOAM predictions and it is sensitive to the near-wall grid cell size. As Fig. 2, b shows, grid refinement brings the predicted gas temperature closer to that measured in the experiments.

a)

b)
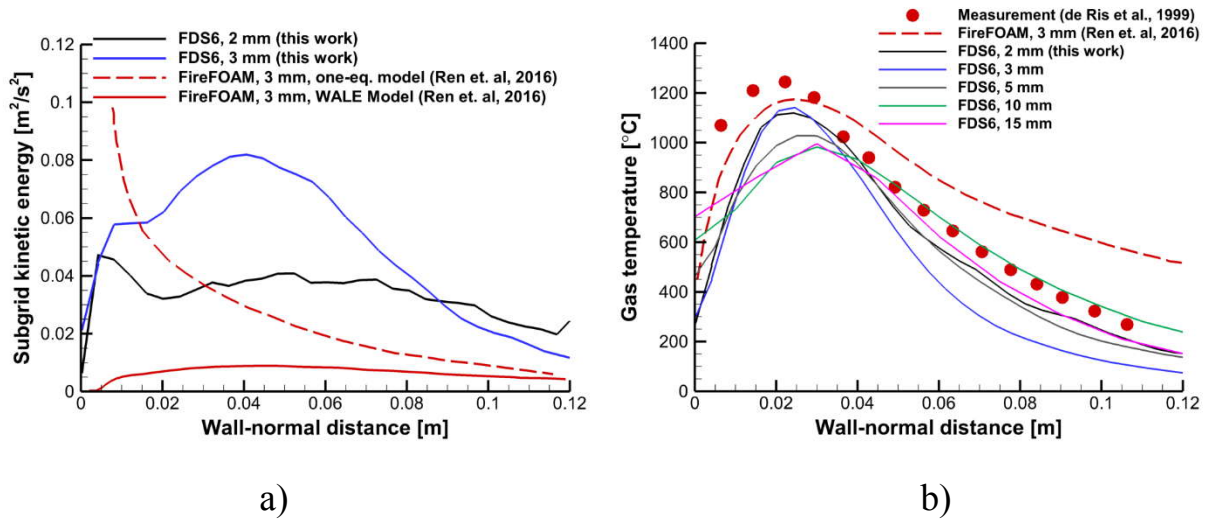
Fig. 2. Time-averaged profiles along wall-normal distance at the centrally located vertical plane, at the elevation of 0.77 m above the burner bottom: a) – subgrid kinetic energy; b) – gas temperature
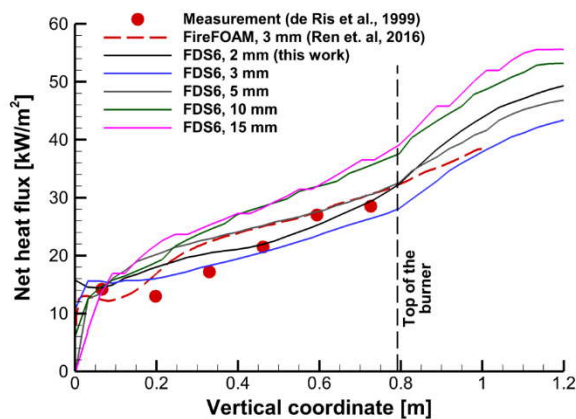
Fig. 3. Time-averaged vertical distributions of the net heat flux along the vertical centerline at the burner surface

Predicted distribution of the net heat flux received from flame by the burner surface favorably agrees with the measurement data (see Fig. 3), provided the mesh is sufficiently fine. It can therefore be concluded that accurate replication of the

boundary layer structure and of surface heat fluxes may require very fine grids with the near-wall grid cell size is of order of few mm. This requirement is very restrictive and is difficult to obey in large-scale practical simulations.

3.2. Upward flame spread over vertical surface

In the simulations of the upward flame spread over vertical surface, the experimental scenario of Ref. [12] is replicated. The PMMA slab having dimensions of 5 m height, 0.6 m wide, 2.5 cm thick was ignited at the bottom (see Fig. 4), and subsequent flame spread dynamics was addressed.
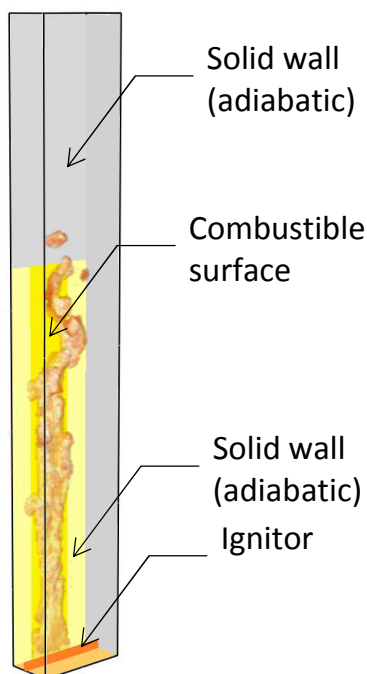
Fig. 4. Computational domain for the upward flame propagation scenario. The instantaneous flame shape is visualized by the iso-surface of heat release rate (200 kW/m^3)

The back side of the combustible slab as well as the solid walls atop and aside of the combustible surface are insulated. Impermeable solid walls are also installed on the side boundaries of computational domain, while its front boundary is set open. The ignitor is represented by the hot plate located at a distance of 0.2 m from the combustible surface (Fig. 4).

For PMMA, extensive experimental data is available on its pyrolysis, ignition and burning. Based on the literature data, thermal conductivity, density, and specific heat

were taken, respectively, k = 0.21 W/(m·K), ρ = 1190 kg/m^3, and c_P = 1.377 kJ/(kg·K). Fuel surface emissivity was set to 0.9. First order reaction with kinetic parameters $A = 8.5 \cdot 10^{12}$ s^{-1}, E_a = 188 kJ/mol was used to simulate pyrolysis reaction rate. Heat of gasification was set 0.87 MJ/kg.

Burning rate at the combustible surface was evaluated by the full coupling of the net heat flux and the pyrolysis rate as highlighted above. The coupled simulations were performed with much coarser grids (16-25 mm) than those in the wall fire case. However, the plume resolution index (the ratio of characteristic buoyant length scale to the grid cell size) was kept above 10, which enables accurate prediction of the buoyant flame.

a)   b)
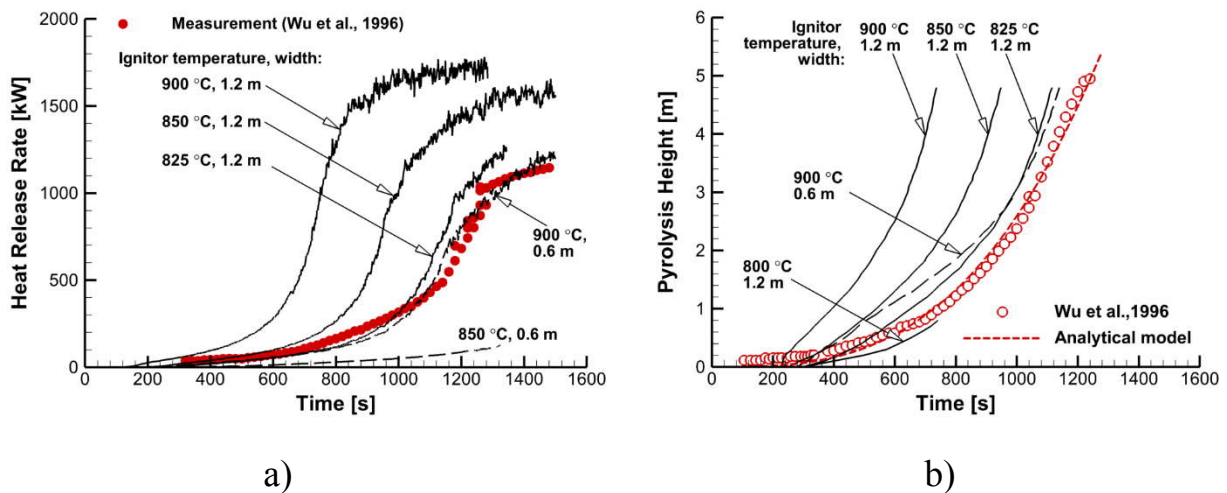
Fig. 5. Flame spread dynamics: a) – heat release rate; b) – pyrolysis height versus time

No complete information on the ignitor properties is given in the description of the prototype experiment, Ref. [12]. In the simulations performed in this work, we varied these properties in the range 0.1–0.3 m (height), 0.6–1.2 m (width), and 800–1300 °C (temperature). As a result, it was found that the flame spread regime is strongly affected by width, height, and surface temperature of the ignitor.

Transient variation of heat release rate and elevation of the pyrolysis front at the centerline is shown in Fig. 5. It appears to be possible to replicate the experimental

results with a reasonable accuracy by adjusting ignitor width and temperature to 0.6 m and 900 °C, respectively. No flame propagation was predicted if the ignitor temperature was reduced to 800 °C, which is the indication that the heat flux produced by the ignitor was reduced below the critical one. It also implies that a relatively small variation in ignitor parameters can lead to either fire growth or fire decay.

Three qualitatively different regimes of flame spread were observed in this work. Depending on the shape of the pyrolysis zone (shown in Fig. 6), we designate these regimes as *necking* (Fig. 6, a), *parabolic* (Fig. 6, b) and *V-shaped* (Fig. 6, c).

a)   b)   c)
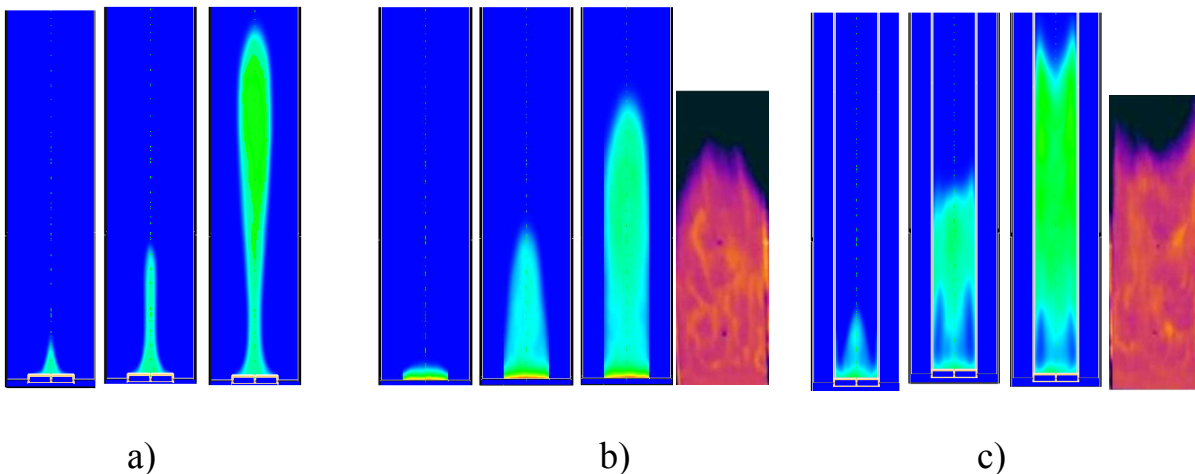
Fig. 6. Instantaneous burning rates (0–6 g/(m^2·s)) at three consecutive time instants and the infra-red flame images from Ref. [15] for three flame propagation regimes: a) – necking, b) – parabolic; c) – V-shaped

The necking regime was observed for low-height (0.1 m), low-temperature (below 1000 °C) ignitor which produced a non-uniform ignited spot at the combustible surface. Absence of the adjacent side walls and intensive side air entrainment become particularly important in this case. The parabolic regime exhibits a typical pyrolysis pattern observed in different experimental scenarios and reported in the literature (for example see [15]). This shape of the pyrolysis front was obtained in FDS simulations for a wide (1.2 m), tall (0.1–0.3 m), high temperature (above 1000 °C) igniter without adjacent side walls. In this case, the incident heat flux at the combustible surface was

more uniformly distributed than that in the necking regime. If the same ignitor as that in the parabolic regime is used and, additionally, vertical side walls are adjacent to the combustible surface, then the shape of flame and of the pyrolysis zone changes. The V-shaped pyrolysis front is then observed, which is explained by the limited side air entrainment and by the recirculating airflow bypassing the side walls. It is worthy of note that the above regimes were predicted numerically before similar observations of the experimental flame shapes, Ref. [15], were found in the literature by the authors of this work.

Thus, both predicted and experimentally observed shapes of the pyrolysis zone cannot be characterized by a rectilinear front. This implies that the heat release rate is not proportional to the pyrolysis height, and it must be taken into account in interpreting the measurement data and applying the simplified analytical models of flame spread.

4. Conclusions

In order to develop the FDS-based methodology of predicting upward flame spread, both uncoupled simulations of vertical wall fire and coupled simulations of upward flame spread over the vertical large scale surface were performed. In the vertical wall fire simulations, the effect of grid resolution and of near-wall modeling on predicted thermal feedback to solid fuel was examined. Reasonable agreement with experimental data and FireFOAM simulation results is observed for the gas temperatures and the heat fluxes incident to the burner surface. We also observed that the effect of the near-wall grid resolution on the net surface heat flux is relatively weak, despite of considerable variation of the resolved temperatures. This is due to the dominating contribution of the radiative flux, which is evaluated based on the pre-assumed radiative fraction.

The flame spread regimes were investigated for a large-scale upward flame spread case. It is found that the ignitor size and temperature as well as the transversal air

entrainment strongly affect the shape of pyrolysis front. As a result, even small variation of the ignitor properties in the near-critical region leads to the qualitative change in the dynamics of the heat release and flame spread velocity. Three distinct flame propagation regimes with necking, parabolic, and V-shaped pyrolysis zones have been identified.

Acknowledgement

References

1. Saito K., Quintiere J. G., Williams F. A. Upward Flame Spread // Fire Safety Science – Proceedings of the First International Symposium. – 1986. – P. 75–86.

2. Hasemi Y. Thermal Modeling of Upward Wall Flame Spread // Fire Safety Science – Proceedings of the First International Symposium. – 1986. – P. 87–96.

3. Delichatsios M. A., Saito K. Upward Fire Spread: Key Flammability Properties, Similarity Solutions and Flammability Indices // Fire Safety Science – Proceedings of the Third International Symposium. – 1989. – P. 217–226.

4. Yan Z., Holmstedt G. CFD Simulation of Upward Flame Spread over Fuel Surface // Fire Safety Science – Proceedings of the Fifth International Symposium. – 1997. – P. 345–356.

5. Lewis MJ., Rubini PA., Moss JB. Field Modelling of Non-Charring Flame Spread // Fire Safety Science – Proceedings of the Sixth International Symposium. – 2000. – P. 683–694.

6. Kwon J.- W., Dembsey N. A., Lautenberger C. W. Evaluation of FDS V.4: Upward Flame Spread // Fire Technology. – 2007. – V. 43. – P. 255–284.

7. Leventon I. T., Li J., Stoliarov S. A flame spread simulation based on a comprehensive solid pyrolysis model coupled with a detailed empirical flame structure representation // Combustion and Flame. – 2015. – V. 162. – P. 3883–3895.

8. Pizzo Y., Lallemand C., Kacem A., Kaiss A., Gerardin J., Acem Z., Boulet P., Porterie B., Steady and transient pyrolysis of thick clear PMMA slabs // Combustion and Flame. – 2015. – V . 162. # 1. – P. 226–236.

9. Kacem A., Mense M., Pizzo Y., Boyer G., Suard S., Boulet P., Parent G., Porterie B. A fully coupled model for open air combustion of horizontally-oriented PMMA samples // Combustion and Flame. – 2016. – V. 170. – P. 135–147.

10. Singh A. V., Gollner M. J. A methodolody for estimation of local heat fluxes in steady laminar boundary layer diffusion flames // Combustion and Flame. – 2015. – V. 162. # 5. – P. 2214–2230.

11. Ren N., Wang Y., Vifayeau S., Trouve A. Large eddy simulation of turbulent vertical wall fires supplied with gaseous fuel trough porous burners // Combustion and Flame. – 2016. – V. 169. – P. 194–208.

12. Wu P.K., Orloff L., Tewarson A. Assessment of Material Flammability with the FSG Propagation Model and Laboratory Test Methods // 13th Joint Panel Meeting of the UJNR Panel on Fire Research and Safety. – 1996. – NIST, Gaithersburg, MD, USA.

13. McGrattan K., McDermott R., Weinschenk C., Hostikka S., Floyd J. K. Over-holt K. Fire Dynamics Simulator Technical Reference Guide. V. 1. Mathematical model. FDS version 6. NIST Special Publication 1019, Sixth ed. – 2015. – 147 P.

14. de Ris J. L., Markstein G. H., Orloff L., Beaulieu P.A. Flame heat transfer. Part I: pyrolysis zone. Technical Report J.I. 0D0J9.MT, Factory Mutual Research Corporation – 1999.

15. Tsai K.-C. Influence of sidewalls on width effects of upward flame spread // FSJ. – 2011. – V. 46. – P. 294–304.